Approximate charge and transition energy cross-section scaling for excitation of atoms colliding with multicharged ions

R. K. Janev
International Atomic Energy Agency, Wagramerstrasse 5, P.O. Box 100, A-1400 Vienna, Austria
(Received 1 June 1995)

Using the adiabatic theory and the dipole close-coupling and classical impulse approximations, scaling relations are derived for the cross sections of dipole-allowed and dipole-forbidden $1\,^1S\rightarrow n\,^1L$ excitation transitions in atoms induced by multiple charged ions of intermediate to high reduced energies. The cross-section scalings incorporate the ionic charge q, the electron transition energy ω_{1n}, and the oscillator strength (in the case of optically allowed transitions). The derived scalings describe well the available experimental data for H and He atoms for reduced energies $E/q\omega_{1n}$ greater than about 25 keV/amu. These scalings also show that, for a fixed energy, the nonscaled excitation cross section as a function of q does not saturate at high q values but decreases after reaching a maximum.

PACS number(s): 34.50.Fa

I. INTRODUCTION

The excitation of atoms in collisions with multiple charged ions A^{q+} $(q\geqslant 2)$ has recently become a subject of increased experimental [1–4] and theoretical [5–12] interest, motivated mainly by the important role of this process in the attenuation dynamics of energetic neutral atom beams injected into fusion plasmas for heating and diagnostic purposes [13,14] and by the so-called "q-saturation" problem of excitation cross sections for a fixed energy with increasing q [15,16]. The most extensive and systematic experimental studies were carried out for the transitions $1\,^1S\rightarrow n\,^1P$ $(n=2-6)$ in H [4] and $1\,^1S\rightarrow n\,^1L$ $(n=2-4,\ L=S,P,D)$ in He [1–3] in the energy range from $\sim 15q$ to $\sim$ (160-200)q keV/amu, with ions of various species in charge states in the range $2\leqslant q\leqslant 45$. These studies have demonstrated that, in the collision energy range investigated, the measured excitation cross sections σ obey (within their experimental uncertainties of 20–30 %) the scaling relationship

$$\frac{\sigma}{q}=f\left(\frac{E}{q}\right), \tag{1}$$

predicted earlier within a three-state close-coupling scheme for the S-P transitions with a dipole approximation for the interaction potential [5]. The multistate close-coupling calculations performed more recently for the $2\,^1P$ excitation of H $(1\,^1S)$ [7,9,11] and the $3\,^1P$,$4\,^1S$,^1P,^1D excitation of He $(1\,^1S)$ [12] also confirm the cross-section scaling (1) in the energy region above (15–20)q keV/amu. The scaling (1) is a direct consequence of the dipole approximation for the interaction potential [10], but follows also from classical dynamics considerations ([1,7], see also below). The physical basis of the scaling relationship (1) lies in the fact that for multiply charged ions the distant collisions give dominant contribution to the excitation process, which justifies the use of dipole potential approximation.

The purpose of the present paper is to derive an approximate scaling for the excitation cross section in atom-multicharged ion collisions which, apart from the ionic charge q, also incorporates the transition energy $\omega_{1n}=|E_1-E_n|$ between the initial and final atomic states. The derivation will be based on the "advanced" adiabatic ("hidden crossings") approach to the low-energy ion-atom collisions [17,18] and on the dipole close-coupling (DCC) and classical impulse (CI) approximations (for the optically allowed and optically forbidden transitions, respectively) for the intermediate to high collision energies. The cross-section scaling relationship we are looking for is of the form

$$\tilde{\sigma}=g(q,\omega_{1n}\xi)\sigma=F(\tilde{E}),\quad \tilde{E}=h(v,q,\omega_{1,n},\eta), \tag{2}$$

where v is the collision velocity, ξ and η collectively designate other parameters of the process and of the collision system (such as the oscillator strength for optically allowed transitions, effective charge of the atomic ion core, etc.), and g and h are functions of their arguments that need to be determined. $\tilde{\sigma}$ and $\tilde{E}$ are the scaled (or reduced) cross section and energy, respectively. Various simple theoretical models, which in limited regions of parameters q, ω_{1n}, ξ, η, and v may adequately describe the collision dynamics of the excitation process, can provide analytic expressions for the functions g, h, and F. The most widely known such models are the adiabatic approximation, classical impulse approximation, and the first Born approximation [19,20]. The trust in the present paper is placed on the possibility to find at least approximate expressions for the scaling functions g and h valid in a broad range of variation of their parameters. While the general form of the function $F(\tilde{E})$ cannot be determined theoretically in the entire reduced energy region, its dominant behavior in the high- and low-$\tilde{E}$ regions can be fairly successfully described by some of the simple theoretical models. The determination of approximate functions g and h is done below separately for the dipole-allowed and dipole-forbidden transitions. Our considerations will also be limited to the case of an $n_0\ ^1S$ initial state.

II. DIPOLE-ALLOWED TRANSITIONS

The three-state DCC approximation [5] for the $n_0s\rightarrow np$ transitions provides a cross-section scaling in the form (2) with

$$g_{\rm DCC}=\frac{\omega_{1n}^2}{qf_{1n}}\lambda,\quad h_{\rm DCC}=\frac{v^2}{q\omega_{1n}\lambda},\quad \lambda=(f_{1n}/2\omega_{1n})^{1/2} \tag{3}$$

and

$$F_{\rm DCC}^{(\rm ad)}(h)\sim\frac{1}{h_{\rm DCC}}\exp(-c_1/h_{\rm DCC}^{1/2}),\quad h_{\rm DCC}\ll h_m,$$

$$F_{\rm DCC}^{(B)}(h)\sim\frac{1}{h_{\rm DCC}}\ln(c_2h_{\rm DCC}),\quad h_{\rm DCC}\gg h_m, \tag{4}$$

where c_1,c_2 are some constants, f_{1n} is the oscillator strength, $h_m(\sim 1)$ is the value of $h_{\rm DCC}$ at which $\tilde{\sigma}$ has its maximum value, and the superscripts (ad) and (B) refer to the adiabatic and the ''Born'' region of h values. Multistate close-coupling calculations [7,9] have demonstrated that the function $F_{\rm DCC}^{(\rm ad)}(h_{\rm DCC})$ does not adequately represent the scaled cross section in the region $h_{\rm DCC}<h_m$. Indeed, the excitation dynamics in this region always includes coupling of many adiabatic molecular states, the number of which increases with the increase of ionic charge. Within the ''advanced'' adiabatic (or ''hidden crossings'') approach to atomic collisions, one of the dominant excitation mechanisms is the evolution of the system along the so-called Q superseries of transition points R_c, which lie in the complex plane of internuclear distance R. (Here we adopt the notation of hidden crossing series given in Ref. [17]. In the case of charge symmetric systems, the Q superseries are denoted T superseries.) During the receding state of the nuclei, the system follows this superseries up to the molecular states which at $R\to\infty$ correlate with the Stark states associated with the final state of the $n_0s\to nl$ transition. The excitation probability is therefore proportional to the product of the elementary transition probabilities at each of the traversed Q-transition points $R_{c,k}^{(Q)}$, i.e. [17],

$$P_{1n}\sim\prod_{k=n_0}^{n}\exp\left(-\frac{2}{v}\Delta_k^{(Q)}(b)\right)=\exp\left(-\frac{2}{v}\sum_{k=n_0}^{n}\Delta_k^{(Q)}(b)\right), \tag{5}$$

where $\Delta_k^{(Q)}$ is the generalized Massey parameter, and b is the impact parameter. Assuming $q\gg 1$ and $(n_0/n)\ll 1$, i.e., that the number of Q-transition points involved in the $n_0\to n$ transition is large, the sum in Eq. (5) can be replaced by an integral; using further the expressions for $\Delta_k^{(Q)}$ from Refs. [17,18], one obtains for the leading term in Eq. (5) [to within an accuracy of $O(n_0^2/n^2)$],

$$P_{1n}\sim\exp\left[-a\frac{(q\omega_{1n})^{1/2}}{v}\left(1+\frac{b^2}{2|R_n^Q|^2}\right)\right],\quad a={\rm const}, \tag{6}$$

where $R_n^{(Q)}$ is the outermost point of the Q superseries involved. After integration over the impact parameters (up to $b={\rm Re}R_n^Q\sim q^{1/2}n^2$), the adiabatic excitation cross section is obtained in the form

$$\sigma^{(\rm ad)}\sim qn^4\frac{v}{(q\omega_{1n})^{1/2}}\chi(v,q,n_0,n)\exp\left(-a\frac{(q\omega_{1n})^{1/2}}{v}\right), \tag{7}$$

where the function $\chi(v,q,n_0,n)$ originates from the unspecified preexponential factor in Eq. (6). Equation (7) contains the correct dominant exponential dependence of σ on the collision velocity and parameters q and ω_{1n}, which implies that the correct form of the reduced energy parameter in the adiabatic region is $h_0=v^2/q\omega_{1n}$. The comparison of this form with $h_{\rm DCC}$ in Eq. (3) indicates that, at least in the adiabatic region, $\lambda=1$. It should be noted that the factor λ from $g_{\rm DCC}$ can be associated with the function $F_{\rm DCC}(h)$ and in the asymptotic regions the presence of λ in $F_{\rm DCC}$ automatically disappears $(h_{\rm DCC}\lambda=h_0)$, except in the argument of the logarithmic function. Therefore, the scaling functions

$$g_0=\frac{\omega_{1n}^2}{qf_{1n}},\quad h_0=\frac{v^2}{q\omega_{1n}} \tag{8}$$

ensure the cross-section scaling for both $h_0<h_m$ and $h_0>h_m$, provided the condition $\ln h_0\gg|\ln\lambda|$ is satisfied. For $(n/n_0)\gg 1$, this condition reduces to $\ln h_0\gg\ln n$.

III. DIPOLE-FORBIDDEN TRANSITIONS

The adiabatic result (7) for $\sigma^{(\rm ad)}$ holds for both dipole-allowed and dipole-forbidden transitions and, therefore, suggests the form of the function h [as given by Eq. (8)]. For determining the scaling function $g(v,q,n,\xi)$ we shall make use of the result for σ for the $n_0\to n$ transitions in a hydrogenlike atom provided by the classical impulse approximation [21],

$$\sigma_{\rm CI}=a\frac{q^2n_0^2n(7n^2-3n_0^2)}{v^2(n^2-n_0^2)^3},\quad a={\rm const}. \tag{9}$$

For a non-hydrogen-like atom, n_0 and n in Eq. (9) have the meaning of effective principal quantum numbers. Introducing the transition energy $\omega_{1n}=2^{-1}(n_0^{-2}-n^{-2})$ and assuming $(n_0/n)^2\ll 1$, Eq. (9) can be written in the form

$$\sigma_{\rm CI}\simeq\frac{q^2}{v^2}\frac{1}{n_0^4}\frac{1}{n_3\omega_{1n}^3},\quad b={\rm const}. \tag{10}$$

If one retains the form of h as given by Eq. (8), then Eq. (10) gives the following forms of the scaling functions:

$$g_{\rm CI}=\frac{n_0^4n^3\omega_{1n}^4}{q},\quad h_{\rm CI}=\frac{v^2}{q\omega_{1n}}(=h_0), \tag{11}$$

with $\tilde{\sigma}_{\rm CI}=bh_{\rm CI}^{-1}$. Since there is at present no theoretical basis for determining g in the adiabatic region, one should assume that $g_{\rm CI}$ can be extended also in the region $h_0<h_m$. This assumption, of course, introduces a large uncertainty and can be verified only *a posteriori*. It should also be noted that the expression (9) for $\sigma_{\rm CI}$ is obtained by summing over the orbital momentum quantum numbers of the initial and final states. Therefore, the scaling functions $g_{\rm CI}$ and $h_{\rm CI}$ should be valid, strictly speaking, only for the $n_0S\to nS$ transitions. However, one can expect that the scaling functions (11) remain valid also for the $n_0S\to nL$ $(L\neq 1)$ transitions, provided L is not too large. It should also be mentioned that the close-coupling calculations of probability for the forbidden transition $1\,^1S\to 2\,^1S$ in He [12]

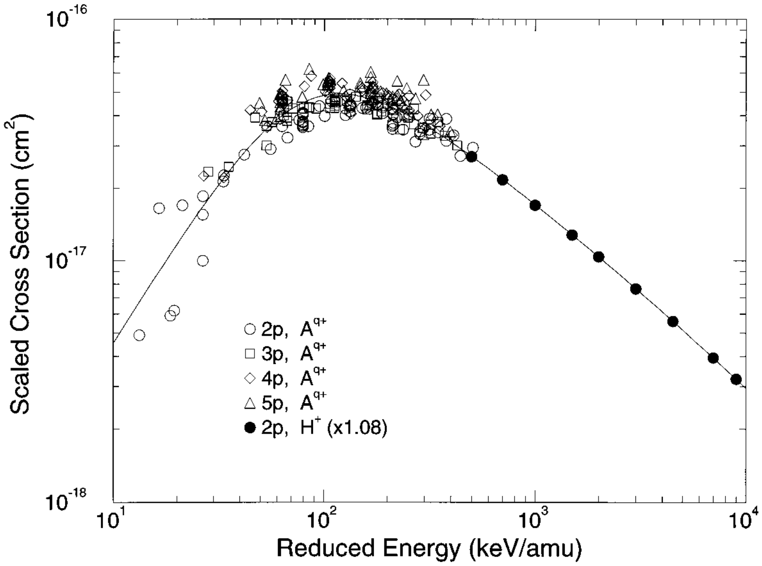

FIG. 1. Scaled excitation cross sections, Eq. (12), for $1s \rightarrow np$ ($n=2$–5) transitions in atomic hydrogen. Open symbols represent the experimental data of Ref. [4] for multicharged ion impact; filled circles are the proton impact data of Ref. [8], multiplied by a factor of 1.08. The solid curve is a fit to the data, Eq. (13).

show a q dependence stronger than q^2 at very large impact parameters. However, in this region of impact parameters the probability is already very small and its contribution to the cross section is not appreciable. This effect is also compensated for by a corresponding reduction of the probability for this transition in the region of smaller impact parameters. We shall now test the derived approximate scalings on the experimental data from Refs. [1–4].

IV. SCALED EXCITATION CROSS SECTIONS FOR H AND He

A. $1\,{}^1S \rightarrow n\,{}^1P$ transitions in H and He

The experimental data for the $1s \rightarrow np$ ($n=2$–5) transitions in H induced by He^{2+}, Si^{q+} ($q=2$–9), and Cu^{q+} ($q=3$–11) ion impact (Ref. [4]) are shown in Fig. 1 in the reduced representation ($\tilde{E}=25h_0$ keV/amu)

$$\tilde{\sigma}=\frac{\omega_{1n}^2}{q f_{1n}}\sigma, \quad \tilde{E}=\frac{E}{q\omega_{1n}} \text{ keV/amu}, \tag{12}$$

where ω_{1n} is expressed in atomic units. We note that the claimed experimental cross-section uncertainties are 25–40 % for the Si^{q+} ions and 16–33% for the Cu^{q+} ions. Within these uncertainties, the data also obey the scaling relationship (12), except for the region $\tilde{E}<30$ keV/amu, where the deviations are large. The solid curve in the figure represents the analytic fit to the data and is given by the equation

$$\tilde{\sigma}(\tilde{E})=\frac{A\,\exp(-\alpha/\tilde{E}_{150}^{1/2})\ln(e+\gamma\tilde{E}_{150})}{(1+C\tilde{E}_{150}^{-\beta})\tilde{E}_{150}}\times 10^{-17}\ \text{cm}^2, \tag{13}$$

where $\tilde{E}_{150}=\tilde{E}/150$, $e=2.718\,282\ldots$, and the values of fitting coefficients are $A=3.65$, $C=0.26$, $\alpha=0.1$, $\beta=2.15$, and $\gamma=3.5$. This function has asymptotic behavior in accordance with Eq. (7) for $\tilde{E}\ll\tilde{E}_m$, and behaves as $\tilde{E}^{-1}\ln\tilde{E}$, for $\tilde{E}\gg\tilde{E}_m$, where $\tilde{E}_m\simeq 120$–150 keV/amu. For $\tilde{E}\geqslant 500$ keV/amu, Eq. (13) describes also the scaled H^+ impact excitation data for $n=2$ of Ref. [8] (obtained with the symmetrized eikonal approximation), increased by 8% to merge the $2p$ experimental data with $q\geqslant 2$ in the reduced energy range 300–500 keV/amu.

The experimental data of Refs. [1–3] for the $1\,{}^1S\rightarrow n\,{}^1P$ ($n=3,4$) transitions in He induced by multicharged ions with $q=2-45$ are shown in Fig. 2. (The uncertainties of the data are 20–30 %). For $\tilde{E}>300$ keV/amu also shown in this figure are the scaled proton impact experimental cross sections for the same transitions taken from Ref. [22], which agree (to within 3–5 %) with the first Born results [23]. The solid curve in Fig. 2 is a fit to the data with an analytic expression of the form (13) and fitting coefficients $A=3.60$, $C=0.31$, $\alpha=0.10$, $\beta=2.15$, and $\gamma=1.7$. The form of the scaled cross section for $1s\rightarrow np$ transitions in He is very similar to that for H, as evidenced by the closeness of the values of fitting parameters and of the energy $\tilde{E}_m$ of the cross-section maximum. In the region of $\tilde{E}$ above 30 keV/amu the ratio $\tilde{\sigma}_{np}(\text{H})/\tilde{\sigma}_{np}(\text{He})$ is almost constant and close to the value $(I_{\text{He}}/I_{\text{H}})^{1/2}\simeq 1.34$, where I_{He} and I_{H} are the ionization potentials of He and H, respectively.

B. $1\,{}^1S\rightarrow n\,{}^1S$ and $1\,{}^1S\rightarrow n\,{}^1D$ transitions in He

The averaged (over their dispersion) experimental cross sections for the $1\,{}^1S\rightarrow n\,{}^1S$ ($n=3$–5) transitions in He taken from Ref. [2] are shown in Fig. 3 in the scaled form [see Eqs. (2) and (11); $\tilde{E}=25h_0$ keV/amu]

$$\tilde{\sigma}=\frac{n^3\omega_{1n}^4}{q}\sigma, \quad \tilde{E}=\frac{E}{q\omega_{1n}} \text{ keV/amu}. \tag{14}$$

In the region above $\tilde{E}=200$ keV/amu, the scaled proton impact experimental data of Ref. [22] for $n=3$ and $n=4$ are also shown, multiplied by a common factor of 0.78 to merge the experimental data with $q\geqslant 2$ in the reduced energy range around 200 keV/amu. The figure shows that for $\tilde{E}>60$ keV/amu the data for the $4\,{}^1S$ excitation are systematically (by about 30%) below those for the $3\,{}^1S$ and $5\,{}^1S$ states.

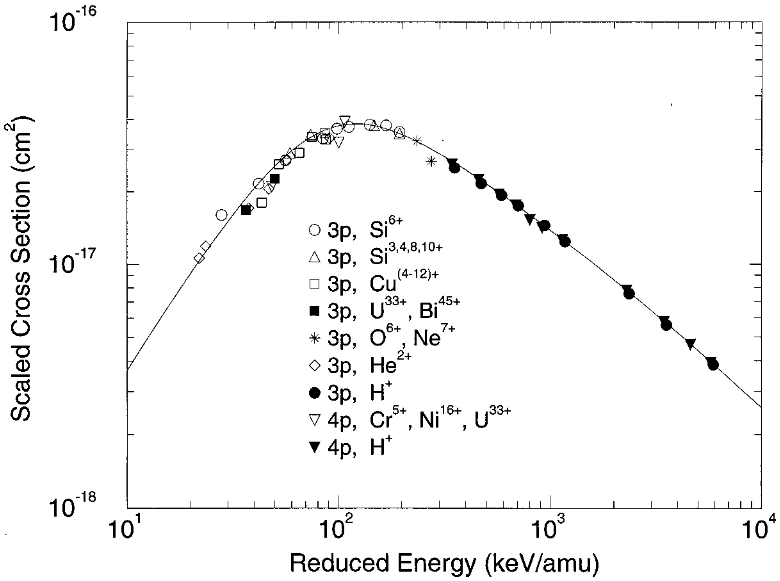

FIG. 2. Scaled excitation cross sections, Eq. (12), for $1\,^1S \rightarrow n\,^1P$ ($n=3,4$) transitions in He. The symbols represent the experimental data of Refs. [1–3], except for the filled circles ($3p$) and filled inverted triangles ($4p$), which represent the experimental proton impact data, Ref. [22]. The solid curve is a fit to the data with Eq. (13).

However, the scaled proton impact $4\,^1S$ excitation cross section does not show this anomaly. If it is not related to some systematic experimental error, the deviation of the scaled $4\,^1S$ cross section for $\tilde{E} > 60$ keV/amu from those for $3\,^1S$ and $5\,^1S$ needs further investigation. The claimed uncertainties of the experimental data for each individual n^1S set of data is about 20%. Within this uncertainty the scaled cross sections in Fig. 3 (except for $4\,^1S$ for $\tilde{E} > 60$ keV/amu) can be represented by the analytic function

$$\tilde{\sigma}(\tilde{E}) = \frac{AB}{B\tilde{E}_{50}^{-\beta}\exp(\alpha/\tilde{E}_{50}^{1/2}) + A\tilde{E}_{50}} \times 10^{-17}\ \text{cm}^2, \quad (15)$$

where $\tilde{E}_{50} = \tilde{E}/50$ and the fitting parameters have the values $A = 4.12$, $B = 2.45$, and $\alpha = 0.1$, and $\beta = 1.7$. This function ensures the proper asymptotic behavior for both $\tilde{E} \ll \tilde{E}_m$ and $\tilde{E} \gg \tilde{E}m$, where $\tilde{E}_m \simeq 50$–60 keV/amu.

The averaged (over the experimental dispersion) data of Refs. [2,3] for the transitions $1\,^1S \rightarrow n\,^1D$ ($n=3$–5) in He are shown in Fig. 4 in the reduced form (14). Plotted on this figure are also the scaled proton impact data (multiplied by a factor of 1.5) from Ref. [22] for the $1\,^1S \rightarrow 4\,^1D$ transition in the region $\tilde{E} > 200$ keV/amu. The solid line in the figure is a fit to the data (having an experimental uncertainty of 20%) with the expression (15) with the values of the fitting parameters $A = 4.81$, $B = 2.45$, $\alpha = 0.15$, $\beta = 15.5$, and an overall

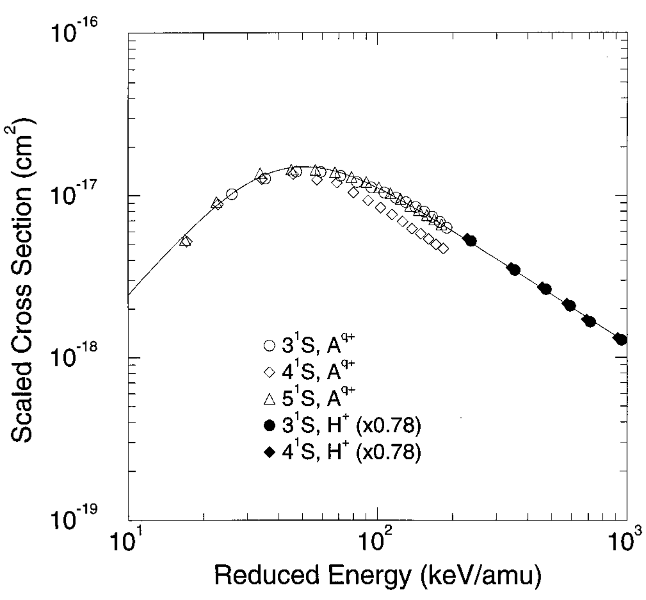

FIG. 3. Scaled excitation cross sections, Eq. (14), for $1\,^1S \rightarrow n\,^1S$ ($n=3$–5) transitions in He. The open symbols represent the experimental data from Refs. [1–3]; the closed symbols are the proton impact data (from Ref. [22]), multiplied by a factor of 0.78. The solid curve is a fit to the data with Eq. (15).

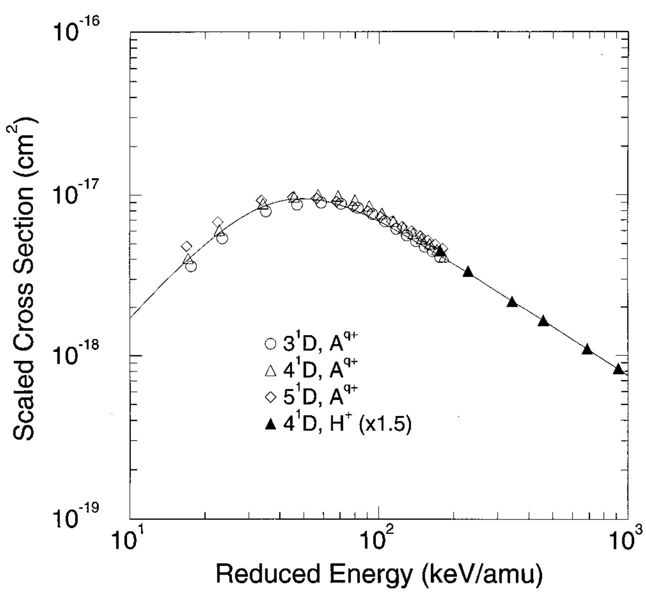

FIG. 4. Scaled excitation cross sections, Eq. (14), for $1\,^1S \rightarrow n\,^1D$ ($n=3$–5) transitions in He. The open symbols are for the experimental data from Refs. [1–3], the closed triangles are the proton impact experimental data for $4\,^1D$ from Ref. [22], multiplied by a factor of 1.5. The solid curve is a fit to the data with Eq. (15).

multiplicative factor of 0.615. The maximum of the scaled cross section appears at the same energy as in the case of $1\,^1S \rightarrow n\,^1S$ transitions ($\tilde{E}_m \simeq 50$–60 keV/amu). In the region $\tilde{E} < \tilde{E}_m$ the experimental data show a weak n dependence (the deviations from the fit are, however, still within the claimed experimental uncertainties of 20%), which originates from the undetermined function $\chi(v,q,n_0,n)$ in Eq. (7). (A similar, but somewhat weaker, n dependence of $\tilde{\sigma}$ can be observed also for the $1s \rightarrow np$ transitions in H in the region $\tilde{E} < \tilde{E}_m$.) In the reduced energy region $\tilde{E} \geqslant 50$ keV/amu, the scaled cross sections $\tilde{\sigma}(^1S)$ and $\tilde{\sigma}(^1D)$ shown in Figs. 3 and 4, respectively, are mutually related by $\tilde{\sigma}(^1D) \simeq 0.615\tilde{\sigma}(^1S)$. The constant ratio of these two scaled cross sections indicates the existence of a (still unrevealed) L scaling of $\tilde{\sigma}(^1L)$ $(L \neq 1)$ in this region.

V. q DEPENDENCE OF THE EXCITATION CROSS SECTION FOR FIXED ENERGY

The scaling relationships (12) and (14), particularly the energy scaling function $h_0 = v^2/q\omega_{1n}$, can be useful in shedding more light on the so-called "saturation" problem for the excitation cross section with increasing q for a fixed collision energy E. The problem has been originally formulated [15,16] within a second-order perturbational approach (using the Schwinger variational principle), and recently investigated in more detail using the finite-difference solution of time-dependent Schrödinger equation [11] and the close-coupling method [12], with a single-center (target) expansion basis in both cases. It is obvious that a perturbational approach that does not simultaneously treat both v^2 and q as large parameters cannot lead to a correct result. Namely, with increasing q for a given (large) value of v^2, one necessarily passes through the region of validity of dipole approximation and thereafter ultimately enters the adiabatic region, where the proper expansion parameter is $v^2/q\omega$. In the adiabatic region, the dominant behavior of the excitation cross section is [cf. Eq. (7)] $\sigma \sim \exp[-a(q\omega_{1n})^{1/2}/v]$ and for a fixed collision velocity σ decreases with increasing q. According to the semiempirical expressions (13) and (15), the decrease of σ with increasing q can be even enhanced by a preexponential factor q^β, with $\beta = 1.15$ or 2.45 for Eqs. (13) and (5), respectively. Therefore, the quasi-independence of the excitation cross section of q takes place in the region of $\tilde{E}$, where neither the perturbational nor he adiabatic description is appropriate (i.e., in the strong-coupling region). Indeed, both the transient q independence and the decrease of σ with increasing q in the adiabatic region of $\tilde{E}$ can be observed already within the three-state DCC approximation. The above remarks on the q behavior of the excitation cross section for a fixed collision energy also apply to the ionization cross section, as it follows from the DCC approximation for ionization [5] and from the correct ionization cross-section scaling in the adiabatic region [24], $\sigma_{\text{ion}} \sim q(v/q^{1/4})\exp(-aq^{1/4}/v)$, for large q.

In Fig. 5 we show the q dependence of the cross section for the transition $1s \rightarrow 2p$ in H for $E = 150$, 300, 600, and 1200 keV/amu. The cross section $\sigma_{2p}(E,q)$ has been determined by fitting Eq. (13) to the experimental data of Ref. [4] for this transition only ($A = 3.65$, $C = 0.39$, $\alpha = 0.08$, $\beta = 2.15$, and $\gamma = 3.5$). The theoretical data of Ref. [11] for $E = 600$ keV/amu are also shown. The figure shows that $\sigma_{2p}(q)$ has a maximum at $q_m \simeq 2.8125E$ keV/amu/$150\omega_{2p}$, which corresponds to the value of reduced energy $\tilde{E} = 53.33$ keV/amu. Since the uncertainty of experimental data in this region is about 30%, the above prediction of q_m also has this uncertainty.

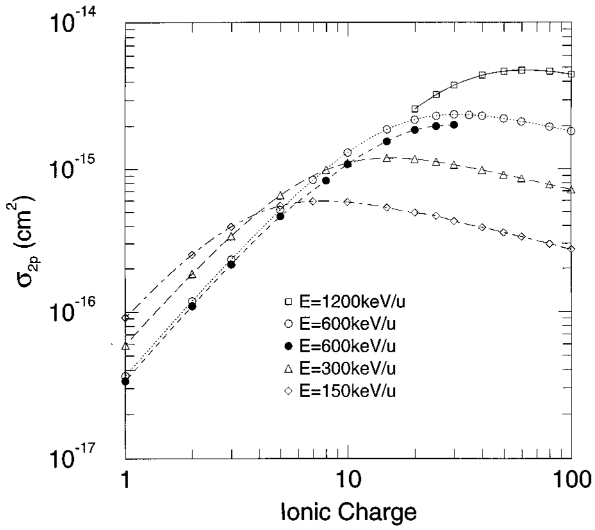

FIG. 5. Ion charge dependence of $1s \rightarrow 2p$ excitation cross section of H. The open symbols are results of the calculated based on Eq. (13), with fitting coefficients determined from the experimental data for this transition. The full circles are the results of calculations in Ref. [11].

VI. CONCLUDING REMARKS

The approximate scalings (12) and (14) for the dipole-allowed and dipole-forbidden transitions, respectively, describe the available experimental data for H and He targets in the region $\tilde{E} > 20$–30 keV/amu rather successfully. The physical assumption underlying these scalings is that for both high and low $\tilde{E}$ there is a dominant excitation mechanism (not necessary direct) connecting the initial and final state. (Fulfillment of this assumption is essential to have ω_{1n} in the denominator of h_0.) For the region $\tilde{E} < \tilde{E}_m$, it has been assumed that the promotion mechanism is the $Q_{1s\sigma}$ superseries of hidden crossings (or an analogous series of avoided crossings, in the case of incompletely stripped ions and/or a many-electron target, such as He). With the decrease of collision energy, however, the population of molecular states correlating with the final atomic state in the excitation process may become possible also through superseries "activated" by rotational or S-type transitions in the united-atom region. If such "indirect" final-state population pathways become dominant in the excitation process, then the parameter ω_{1n} in h_0 should be replaced by ω_{in}, where i designates the initial state of a superseries of crossings. Besides introducing the need for redefining h_0 in such situations, these excitation mechanisms may introduce additional q and n dependences in the g and h scaling functions and even generate structures (new maxima) in the reduced excitation cross section in the low-$\tilde{E}$ region [7,9]. The large deviations in $\tilde{\sigma}(^1P)$ for H in the region $\tilde{E}<30$ keV/amu (see Fig. 1) and the small shoulder around $\tilde{E}=30$ keV/amu in $\tilde{\sigma}(^1P)$ for He in Fig. 2 could have such origin.

The comparison of scaled cross sections $\tilde{\sigma}(^1P)$ for H and He indicates a target core effect on the cross-section value. The incorporation of this effect in the scaling needs further investigation. The scaled cross sections $\tilde{\sigma}(^1S)$ and $\tilde{\sigma}(^1D)$ for He also indicate existence of an L scaling of scaled cross sections for forbidden transitions in the reduced energy region above $\tilde{E}\simeq 50$ keV/amu, which still needs to be revealed.

---

[1] K. Reymann, K.-H. Schartner, and B. Sommer, Phys. Rev. A **38**, 2290 (1988).

[2] M. Anton, D. Detleffsen, and K.-H. Schartner, Nucl. Fusion Suppl. **3**, 51 (1992).

[3] M. Anton, D. Detleffsen, K.-H. Schartner, and A. Werner, J. Phys. **26**, 2005 (1993).

[4] D. Detleffsen, M. Anton, A. Werner, and K.-H. Schartner, J. Phys. B **27**, 4195 (1994).

[5] R. K. Janev and L. P. Presnyakov, J. Phys. B **13**, 4233 (1980).

[6] H. Ryufuku, Phys. Rev. A **25**, 720 (1982).

[7] W. Fritsch and K.-H. Schartner, Phys. Lett. **126A**, 17 (1987).

[8] C. O. Reinhold, R. E. Olson, and W. Fritsch, Phys. Rev. A **41**, 4837 (1990).

[9] W. Fritsch, in *Proceedings of the VIth International Conference on the Physics of Highly Charged Ions*, edited by P. Richard, M. Stocki, C. L. Cocke, and C. D. Lin, AIP Conf. Proc. No. 274 (AIP, New York, 1993), p. 24.

[10] V. D. Rodriguez and J. E. Miraglia, J. Phys. B **25**, 2037 (1992).

[11] V. D. Rodriguez and A. Salin, J. Phys. B **25**, L467 (1992).

[12] F. Martin and A. Salin, J. Phys. B **28**, 671 (1995).

[13] R. K. Janev, Comments At. Mol. Phys. **26**, 83 (1991).

[14] H. P. Summers, M. von Hellmann, F. J. de Heer, and R. Hoekstra, Nucl. Fusion Suppl. **3**, 7 (1992).

[15] B. Brendlé, R. Gayet, J. P. Rozet, and K. Wohrer, Phys. Rev. Lett. **54**, 2007 (1985).

[16] R. Gayet and M. Bouamoud, Nucl. Instrum. Methods B **42**, 515 (1989).

[17] E. A. Solov'ev, Usp. Fiz. Nauk **157**, 437 (1989) [Sov. Phys. Usp. **32**, 228 (1989)].

[18] M. Pieksma and S. Yu. Ovchinnikov, J. Phys. B **24**, 2699 (1991); **25**, L373 (1992).

[19] I. C. Percival and D. Richards, Adv. At. Mol. Phys. **11**, 2 (1975).

[20] R. K. Janev, L. P. Presnyakov, and V. P. Shevelko, *Physics of Highly Charged Ions* (Springer-Verlag, Berlin, 1985).

[21] G. I. Ivanovski and E. A. Solov'ev, Zh. Éksp. Teor. Fiz. **104**, 3928 (1993) [Sov. Phys. JETP **77**, 887 (1993)].

[22] F. J. de Heer, R. Hoekstra, and H. P. Summers, Nucl. Fusion Suppl. **3**, 47 (1992).

[23] K. L. Bell, D. J. Kennedy, and A. E. Kingston, J. Phys. B **1**, 1037 (1968).

[24] R. K. Janev, G. Ivanovski, and E. A. Solov'ev, Phys. Rev. A **49**, R645 (1994).